Molecular Biology of the Cell
Vol. 18, 594–604, February 2007

Mitogen-activated Protein Kinase Kinase 1-dependent Golgi Unlinking Occurs in G_2 Phase and Promotes the G_2/M Cell Cycle Transition[D] [V]

Timothy N. Feinstein and Adam D. Linstedt

Department of Biological Sciences, Carnegie Mellon University, Pittsburgh, PA 15213

Submitted June 19, 2006; Revised November 22, 2006; Accepted November 30, 2006
Monitoring Editor: Benjamin Glick

Two controversies have emerged regarding the signaling pathways that regulate Golgi disassembly at the G_2/M cell cycle transition. The first controversy concerns the role of mitogen-activated protein kinase activator mitogen-activated protein kinase kinase (MEK)1, and the second controversy concerns the participation of Golgi structure in a novel cell cycle "checkpoint." A potential simultaneous resolution is suggested by the hypothesis that MEK1 triggers Golgi unlinking in late G_2 to control G_2/M kinetics. Here, we show that inhibition of MEK1 by RNA interference or by using the MEK1/2-specific inhibitor U0126 delayed the passage of synchronized HeLa cells into M phase. The MEK1 requirement for normal mitotic entry was abrogated if Golgi proteins were dispersed before M phase by treatment of cells with brefeldin A or if GRASP65, which links Golgi stacks into a ribbon network, was depleted. Imaging revealed that unlinking of the Golgi apparatus begins before M phase, is independent of cyclin-dependent kinase 1 activation, and requires MEK signaling. Furthermore, expression of the GRASP family member GRASP55 after alanine substitution of its MEK1-dependent mitotic phosphorylation sites inhibited both late G_2 Golgi unlinking and the G_2/M transition. Thus, MEK1 plays an in vivo role in Golgi reorganization, which regulates cell cycle progression.

INTRODUCTION

Mitogen-activated protein kinase kinase (MEK)1 belongs to the p42/p44 mitogen-activated protein (MAP) kinase pathway, whose canonical role is to transduce cellular responses to mitogenic signals (Roovers and Assoian, 2000). GTP-bound Ras activates Raf1 kinase and assembles Raf, the dual specificity kinases MEK1/2 and the p42/p44 MAP kinases extracellular signal-regulated kinase (ERK)1/2 into a membrane-bound phosphorylation cascade in which Raf1 phosphorylates MEK1/2, which in turn activate ERK, which is then released from the complex and translocates to the nucleus and other cellular sites (Besson *et al*., 2001; Lou *et al*., 2004; Torii *et al*., 2004b). Active nuclear ERK promotes the transcription of D-type cyclins and the cyclin-dependent kinase inhibitor p21Cip1, constituting a necessary step in G_1 exit and S-phase entry.

MEK1 also functions during mitosis. In mitotic *Xenopus* egg extracts, MEK is active and required for normal mitotic progression (Abrieu *et al*., 1997; Walter *et al*., 1997; Bitangcol *et al*., 1998; Murakami and Vande Woude, 1998). MEK inhibition causes defects in both spindle formation (Horne and Guadagno, 2003) and spindle checkpoint control (Minshull *et al*., 1994; Takenaka *et al*., 1997; Chung and Chen, 2003). MEK1 is also active during mammalian somatic cell mitosis (Shapiro *et al*., 1998; Colanzi *et al*., 2000; Hayne *et al*., 2000; Roberts *et al*., 2002). Activation is independent of extracellular growth factor input (Dangi and Shapiro, 2005), and inhibition causes spindle defects (Horne and Guadagno, 2003). Additionally, interfering with MEK1 signaling via expression of dominant-negative mutants, use of chemical inhibitors, or RNA interference (RNAi) significantly delays mitotic entry (Wright *et al*., 1999; Roberts *et al*., 2002; Liu *et al*., 2004), suggesting the existence of a novel mitotic target of MEK-mediated signaling that promotes mitotic entry.

Surprisingly, one apparent mitotic target of MEK1 is the mammalian Golgi apparatus (Acharya *et al*., 1998). The Golgi consists of a contiguous network of laterally linked ministacks positioned at the microtubule-organizing center. During mitosis the Golgi reversibly disassembles. First, lateral connections between ministacks become disrupted, and then the unlinked ministacks undergo extensive vesiculation (Lucocq *et al*., 1987; Misteli and Warren, 1995; Jesch and Linstedt, 1998). Reassembly is initiated in daughter cells at about the time of cytokinesis. Mitotic Golgi disassembly can be induced in permeabilized cells by using mitotic cytosol, and, under these conditions, MEK1 and Raf1 are required components (Acharya *et al*., 1998; Kano *et al*., 2000; Colanzi *et al*., 2003b). Active MEK/ERK complexes are in fact present on the Golgi due to their association with Golgi-localized Sef (Torii *et al*., 2004a). Furthermore, at least one Golgi-localized MEK pathway substrate has been identified, the putative Golgi structural protein GRASP55, and its phosphorylation occurs specifically at mitosis (Jesch *et al*., 2001a). Importantly, however, confirmation of the in vivo role of MEK1 in mitotic Golgi disassembly is lacking and its role has been challenged by several observations. In intact cells, mitotic Golgi disassembly seems normal after inhibiting the ability of MEK to activate ERK (Lowe *et al*., 1998) even when Golgi disassembly is prematurely induced by constitutive cyclin-dependent kinase (CDK) I activation (Draviam *et al*., 2001).

This article was published online ahead of print in *MBC in Press* (http://www.molbiolcell.org/cgi/doi/10.1091/mbc.E06–06–0530) on December 20, 2006.

[D] [V] The online version of this article contains supplemental material at *MBC Online* (http://www.molbiolcell.org).

Address correspondence to: Adam D. Linstedt (linstedt@andrew.cmu.edu).

ERK activation by MEK is also dispensable in a cell free assay in which mitotic cytosol is used to cause disassembly of purified Golgi stacks (Lowe *et al*., 1998). Although it may be that these tests failed to inhibit a novel MEK1 activity (Colanzi *et al*., 2000), another explanation is that MEK1 facilitates, but is not required for, Golgi disassembly (Jesch *et al*., 2001a; Puthenveedu and Linstedt, 2001b). Results in the permeabilized cell assays are most consistent with MEK1 triggering Golgi unlinking and CDK1 triggering Golgi vesiculation (Kano *et al*., 2000). In vivo, vesiculation alone may be sufficient to yield Golgi breakdown that seems normal.

Intriguingly, if MEK1-mediated Golgi unlinking, which has not yet been substantiated in vivo, were to occur before G_2/M, it might explain the aforementioned G_2/M delay induced by MEK inhibition. That is, MEK inhibition might block a rearrangement in the Golgi apparatus that somehow controls G_2/M kinetics. Indeed, a remarkable finding by Malhotra and colleagues (Sutterlin *et al*., 2002), now supported by others (Hidalgo Carcedo *et al*., 2004; Preisinger *et al*., 2005; Yoshimura *et al*., 2005), indicates that Golgi disassembly is required for G_2/M progression. Antibody or dominant-negative interference of GRASP65 blocks mitotic Golgi disassembly in permeabilized cells and when these agents are introduced into intact cells, the cells fail to exit G_2 (Sutterlin *et al*., 2002). The mechanism, however, is unclear. Our recent work indicates that GRASP65 is required for lateral linking of Golgi ministacks (Puthenveedu *et al*., 2006); thus, the previous antibody and dominant-negative treatments may have blocked Golgi unlinking triggered by a signal in late G_2. GRASP65 is mitotically phosphorylated by CDK1 and not MEK1/ERK (Wang *et al*., 2003; Yoshimura *et al*., 2005), which is puzzling given the association of MEK signaling with Golgi unlinking. Alternatively, the identification of GRASP65 as Golgi linking factor suggests that the related GRASP55, which as mentioned above is a MEK/ERK target, may have a similar role. Thus, in late G_2, MEK pathway phosphorylation might regulate GRASP55 such that, although not required for Golgi disassembly, the Golgi becomes unlinked and this is a prerequisite for timely G_2/M. Consistent with this, a recent study shows that an isoform of ERK, ERK1c, controls both mitotic Golgi fragmentation and mitotic progression (Shaul and Seger, 2006). However, this study did not demonstrate that ERK1c induces Golgi disassembly before prophase nor that such Golgi disassembly is a prerequisite for mitotic entry. Furthermore, it did not identify a target of ERK1c involved in Golgi structure and Golgi structural changes necessary for mitotic progression.

Therefore, we first inhibited MEK1 and assayed G_2/M progression in the presence or absence of an assembled, linked Golgi apparatus. Next, we assessed the influence of MEK signaling on Golgi structure in both G_2 and M phase. We also expressed a nonphosphorylatable GRASP55 to test the role of GRASP55 phosphorylation in Golgi structure and G_2/M progression. The combined results confirm an in vivo role for MEK1 in the control of mitotic Golgi reorganization and identify MEK1 signaling as a key component of the putative Golgi "checkpoint."

MATERIALS AND METHODS

Reagents and Cell Culture

Primary antibodies used were as follows: anti-ERK2 C16 (Santa Cruz Biotechnology, Santa Cruz, CA), anti-GPP130 (Bachert *et al*., 2001), anti-p115 (Puthenveedu and Linstedt, 2001a), anti-GRASP65 (Wang *et al*., 2003), diphospho-specific anti-ERK1/2 (Santa Cruz Biotechnology), anti-hemagglutinin (HA) (Bachert *et al*., 2001), anti-Myc 9e10 (Jesch *et al*., 2001a), and anti-giantin (Linstedt and Hauri, 1993). Secondary antibodies were affinity purified and fluorescein isothiocyanate or rhodamine isothiocyanate conjugated (Invitrogen, Carlsbad, CA). Hoechst 33258 and brefeldin A were obtained from Sigma-Aldrich (St. Louis, MO). U0126 was obtained from Promega (Madison, WI), and olomoucine II was from EMD Biosciences (Darmstadt, Germany). Monolayer HeLa cells were cultured in Eagle's minimum essential medium supplemented with 10% fetal bovine serum, 100 U/ml penicillin G, and 100 μg/ml streptomycin. Cells were grown at 37°C and 5% CO_2 in a humidified chamber.

Transfections

HA-MEK1 (Mansour *et al*., 1994) was cloned into pRevTRE (Clontech, Mountain View, CA). Following the manufacturer's guidelines, viral supernatants were collected from transiently transfected RetroPack cells (Clontech) and used to create stable cells expressing HA-MEK1. To induce expression of HA-MEK1, 1 μg/ml doxycycline was added 48 h before analysis. For RNAi, transfection was performed on 35-mm plates according to manufacturer's recommendations (Invitrogen) by using 8 μl of Oligofectamine and small interfering RNA (siRNA) at final concentrations of 30 nM (GM130), 40 nM (MEK1 and MEK2), or 80 nM (GRASP65). After 24 h, the cells were either refreshed with 500 μl of medium and 10% serum, or else medium was rinsed in phosphate-buffered saline (PBS) and changed for the purposes of thymidine washout. Assays were performed at 72 or 96 h posttransfection, as indicated. siRNA oligonucleotides were obtained as purified duplexes from QIAGEN (Valencia, CA). Human MEK1 and MEK2 were targeted with 5′-AAGATTCTACTCTTGTCATTT-3′ and 5′-AAACCACACCTTCATCAAGCG-3′, respectively. GRASP65 was targeted with 5′-AAGGCACTACTGAAAGC-CAAT-3′. Myc-epitope–tagged GRASP55 and GRASP55$_{T222A,T225A}$ (Jesch *et al*., 2001a) were transfected into HeLa cells by using Transfectol (GeneChoice, Frederick, MD) according to the manufacturer's recommendations.

ERK Phosphorylation Assay

Cells were grown to 90% confluence on 35-mm dishes. U0126 (10 μM) or 0.1% DMSO was added for 30 min, and then growth medium was replaced with either hyposaline buffer (20 mM HEPES, 60 mM NaCl, and 2.5 mM Mg acetate) for 5 min or else a brief rinse in PBS. Cells were lysed (1% SDS, 50 mM Tris-Cl, pH 6.8, and phenylmethylsulfonyl fluoride), and protein concentration was assayed using bicinchoninic acid as recommended by the manufacturer (Pierce Chemical, Rockford, IL). Samples (50 μg) were analyzed by immunoblotting using the diphospho-specific monoclonal anti-ERK (at 1:200). Blots were stripped (1 M glycine, pH 2.5, and 0.05% Tween 20 for 30 min at room temperature) and reprobed using the polyclonal anti-ERK2 antibody (at 1:1000). Quantification of signals from enhanced chemiluminescence (Pierce Chemical) was carried out using an LAS-3000 gel imager (Fuji, Stamford, CT).

S-Phase Synchronization and Cell Cycle Studies

For morphological and mitotic index analysis of synchronized cells, the cells were plated at 60% confluence in 35-mm dishes. For double thymidine arrest, cells were maintained in growth medium plus 2 mM thymidine for 24 h and then rinsed and maintained in growth medium for 14 h. Cells were maintained in thymidine for an additional 20 h before final release. After release, cells were assayed for mitotic index by tallying the number of cells displaying clear mitotic (rounded perimeter, discernible mitotic plate) and interphase characteristics by using an inverted microscope and a 20× phase contrast objective. Rare cells displaying abnormal or clearly apoptotic characteristics were not counted. To minimize temperature changes, 200–300 cells were counted in <2 min. When double thymidine arrest was performed along with RNAi, siRNA was applied at the same time as the first application of thymidine and the experiment proceeded otherwise as normal. Consequently, the final thymidine arrest was initiated on day 2 of knockdown before significant loss of protein, and the experiment was carried out on day 3 of knockdown when protein loss was maximal. Single thymidine arrest was used for MEK1 knockdown experiments. Arrest was initiated 18 h post-siRNA transfection and continued for 48 h before release. This ensured passage through the G_1/S transition before knockdown. Where indicated, BFA was added 5 h after release at a final concentration of 2 μM. In experiments involving cell cycle progression in unsynchronized populations, cells were passed to a confluence of 30–40% and maintained for 48 h before addition of U0126 or 0.1% DMSO carrier, followed, where indicated, by addition of 2 μM BFA 2 h later. Where indicated, olomoucine II was added to a final concentration of 10 μM at 6 h after thymidine release, and analysis or washout was performed at 11 h.

To assay MEK activity in synchronized cells, mitotic shake-off was carried out on cultures enriched by double-thymidine synchronization at the point of mitotic entry. Shake-off was performed by rinsing the cells one time in ice-cold shake-off buffer (PBS + 1 mM EDTA) in a refrigerated room, aspirating the supernatant, and striking the culture dish vigorously 10 times against the countertop. Released cells were collected by rinsing with cold shake-off buffer, and the efficiency of release of mitotic cells was estimated >90% by phase-contrast microscopy. Adherent cells, taken to be in late G_2 were then collected by scraping into shake-off buffer. Adherent and mitotic cells were rinsed one time by centrifugation, resuspended in hot sample buffer, and analyzed for phospho-ERK levels as described above.

Microscopy and Image Analysis

Microscopy was performed using an epifluorescence microscope with a 40× oil immersion lens (Linstedt *et al.*, 1997), or a spinning disk confocal system with a 100× oil immersion objective (Puthenveedu *et al.*, 2006), or a fluorescence bleaching-equipped epifluorescence microscope with a 100× oil immersion objective (Puthenveedu *et al.*, 2006). Z-axis sectioning was at 0.3 μm, and images were analyzed after maximum-value projection. Live imaging was performed at 37°C in Opti-MEM (Invitrogen) containing 10% serum. For evaluating the mean number of objects per Golgi, random epifluorescence fields of view were collected using Hoechst DNA staining or phospho-Histone H3 staining rather than the Golgi channel for selection. Images for a given experiment were captured using fixed parameters, and no modifications were performed between capture and analysis with ImageJ software (http://rsb.info.nih.gov/ij/). The images were thresholded using the auto-threshold feature and the number of objects per Golgi was determined using the Analyze Objects feature with a minimum size cutoff of 15 pixels. At least 100 Golgi were assayed per sample, and assays were performed at least three separate times per treatment. For fluorescence recovery after photobleaching, part of the Golgi was bleached using a single laser pulse, and images were acquired every 3 s as described previously (Puthenveedu *et al.*, 2006). Fluorescence values in the bleached and an adjacent nonbleached area were measured using NIH Image. Fluorescence recovery is represented as the ratio of the bleached region to an adjacent unbleached region, normalized to the prebleach and immediate postbleach values.

Statistical Analysis

The statistical significance of all comparisons was assessed by two-tailed Student's *t* tests, and, where indicated, nonoverlap of curves was estimated using root mean squared deviation.

RESULTS

MEK1 Knockdown Delays Mitotic Entry

Due to concerns regarding the effectiveness of pharmacological MEK1 inhibitors in blocking all MEK1-dependent functions, for example, cellular roles that might be noncatalytic or otherwise inhibitor resistant (Colanzi *et al.*, 2000; Harding *et al.*, 2003; however, see Shapiro *et al.*, 1999; Hayne *et al.*, 2004), we used siRNA-mediated knockdown of expression. Using a siRNA duplex targeting the 3′ untranslated region, we observed ~95% knockdown of a stably expressed HA-tagged version of MEK1 in HeLa cells by immunofluorescence (our unpublished data) and immunoblotting (Figure 1A). To confirm knockdown and effective inhibition of the classical catalytic activity, we assayed ERK activation (Itoh *et al.*, 1994). As expected, control cells treated with hyposaline buffer showed a dramatic increase in levels of phospho-ERK peaking at ~5 min (our unpublished data). Using the 5-min time point, it was then observed that ERK activation was attenuated by >50% in cells after MEK1 knockdown (Figure 1B). ERK is also activated by the more abundant MEK2 and indeed siRNA-mediated knockdown of MEK2 inhibited ERK activation still more effectively than depletion of MEK1. Simultaneous MEK1 and MEK2 knockdown was most effective and abolished the ERK activation induced by hyposaline treatment. It is noteworthy that even double-knockdown did not eliminate resting levels of phospho-ERK, whereas the small molecule MEK1/2 inhibitor U0126 did so.

To test the role of MEK1 protein in G_2/M progression, control and knockdown cells were blocked at S phase, and the mitotic index was determined at time points after release. To prevent complications at G_1/S, cell synchronization was carried out such that MEK1 knockdown occurred after the S-phase arrest and before release. Cells treated with a control siRNA passed through mitosis in a cohort that peaked at 8 h (Figure 2A, circles), whereas cells depleted of MEK1 were significantly delayed (Figure 2A, triangles). Values reported are averages of at least three experiments. Consistent with participation of the canonical catalytic activity of MEKI, these results were recapitulated with pharmacological inhibition. U0126 addition delayed the mitotic index peak by 2 h (Figure 2B). There was a difference, however, in mitotic exit. Cells treated with U0126 progressed out of M phase within 1–2 h, whereas MEK1-depleted cells did not. Knockdown of MEK2 did not delay mitotic entry, which is consistent with evidence for nonoverlapping MEK1 and MEK2 roles (Ussar and Voss, 2004).

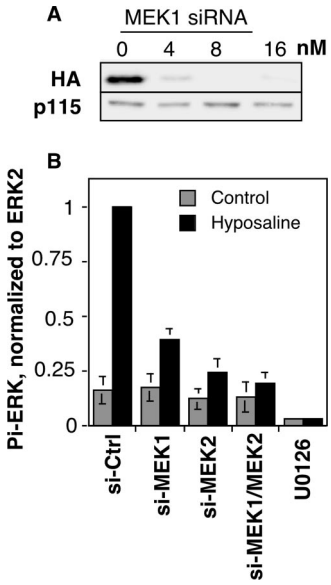

Figure 1. Depletion of MEK1 inhibits ERK activation. (A) Extracts of HeLa cells stably expressing an HA-tagged copy of human MEK1 (40 μg/lane) were prepared 72 h after transfection with the indicated concentrations of the MEK1 siRNA and were analyzed by immunoblotting by using anti-HA to detect HA-MEK1 (top) or anti-p115 as a loading control (bottom). (B) To assay ERK activation after knockdown, HeLa cells were transfected with the indicated siRNAs, and after 72 h, the cells were placed for 5 min in either iso-osmotic buffer (control) or hypo-osmotic buffer (hyposaline). Cell extracts were then prepared and analyzed by immunoblot by using anti-phospho-ERK antibody, and, after stripping of the blot, anti-ERK2 antibody. Quantification of the phospho-ERK/ERK2 ratio is shown (mean ± SEM, n = 3). Note that knockdown, especially the combined MEK1/MEK2 knockdown, blocked stimulated, but not resting, levels of ERK phosphorylation. As a positive control, the phospho-ERK/ERK2 ratio is also shown for cells treated with U0126 for 30 min before the buffer challenges.

As an independent assay not involving cell cycle synchronization, we added U0126 to unsynchronized cells and evaluated mitotic entry. A significant and transient decrease in mitotic cells was observed 2–5 h after addition of U0126 but not DMSO carrier (Figure 2C). After an initial decrease in mitotic cells, a return to close to steady state is the expected result if it is entry into M phase that is altered rather than progression through M phase. Thus, MEK1 inhibition by knockdown or U0126 addition delays, but does not block, G_2/M.

Unlinking the Golgi Apparatus Bypasses the MEK1 Requirement for Normal Mitotic Entry

A G_2/M delay upon MEK1 inhibition is consistent with the possibility that MEK1 unlinks the Golgi as a prerequisite for timely G_2/M. To test this possibility, we first asked whether dispersal of Golgi membranes by using BFA would bypass the MEK requirement. BFA is a noncompetitive inhibitor of Arf1-guanine-nucleotide exchange factor (GEF) that causes redistribution of Golgi components to the endoplasmic reticulum (ER) and vesicular tubular clusters (Lippincott-

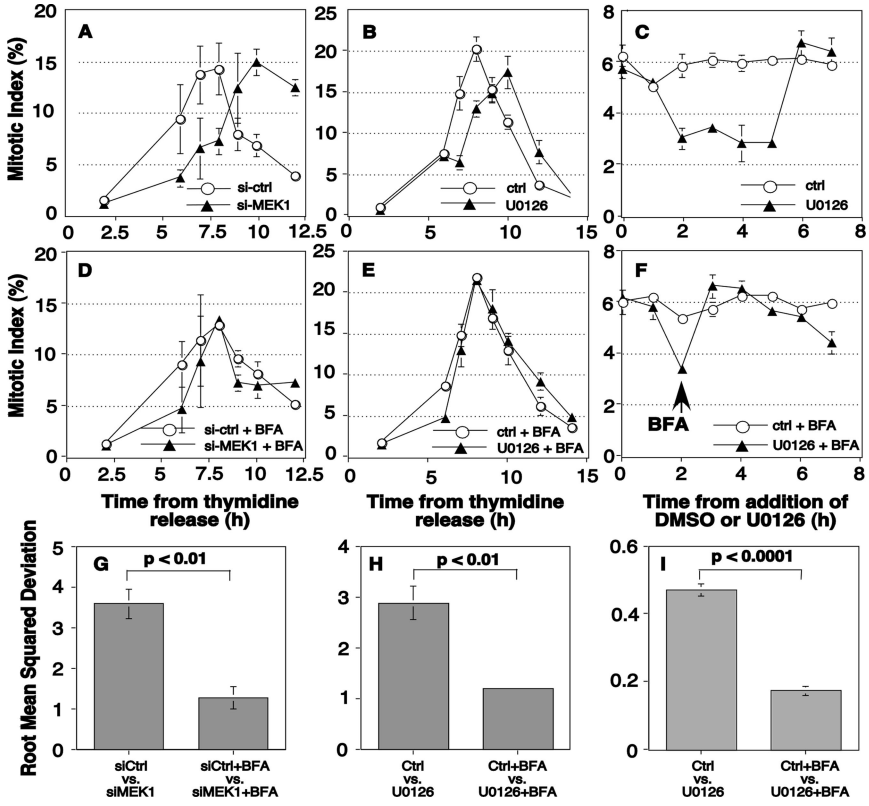

Figure 2. MEK1 promotes mitosis via Golgi disassembly. (A–C) The percentage of cells in mitosis (mitotic index) at the indicated times after thymidine release was determined for control and MEK1 siRNA-transfected cells (A) and control and U0126-treated cells (B). The mitotic index was also determined for unsynchronized cells after addition of U0126 for the indicated times (C). For knockdown cells, a double thymidine S-phase arrest protocol was used in which the first 24-h arrest was initiated upon transfection and lasted 24 h, and the second arrest was initiated after a 14-h incubation in the absence of thymidine and lasted 20 h. For U0126, treatment was initiated 2 h after thymidine release and consisted of growth media containing 10 μM U0126 and 0.1% DMSO or 0.1% DMSO alone. (D–F) To test whether delay required an intact Golgi apparatus, BFA treatment was used to disassemble the Golgi apparatus and the mitotic index was determined for synchronized MEK1 knockdown cells (D), synchronized U0126 treated cells (E), and nonsynchronized U0126 treated cells (F). For synchronized cells 2 μM BFA was added 5 h postthymidine release. For nonsynchronized cells, 2 μM BFA was added 2 h after U0126 addition (arrow). Note that in each assay MEK inhibition delayed mitotic entry and that BFA suppressed the delay. All values shown are averages ± SEM (n ≥ 3). (G–I) The mitotic progression data were analyzed using RMSD to quantify the degree to which the shown mitotic progression curves differ from one another. Results are shown for comparisons between control and MEK1 knockdown-synchronized cells (G), control and U0126-treated synchronized cells (H), and control and U0126-treated nonsynchronized cells (I). In the absence of BFA, significant differences caused by MEK inhibition were evident, and these differences were reduced by >50% in the presence of BFA.

Schwartz *et al*., 1989; Peyroche *et al*., 1999; Seemann *et al*., 2000). Strikingly, treatment of cells with BFA abrogated the 2-h delay caused by either MEK1-knockdown (Figure 2D) or U0126 treatment (Figure 2E). Bypass of the MEK requirement was also observed in unsynchronized cells (Figure 2F). The MEK-induced delay, and its rescue, was further quantified by determining the root mean squared deviation (RMSD) value for each respective time-series (Figure 2, G–I). RMSD values comparing mitotic indices in the presence or absence of MEK1 knockdown or the presence or absence of U0126 were threefold higher than the corresponding comparisons in the presence of BFA. A similar result was obtained for unsynchronized cells.

In contrast to the dramatic dispersal of Golgi components induced by BFA, MEK1-induced Golgi breakdown in permeabilized cells seems to yield relatively large Golgi fragments (Acharya *et al*., 1998; Kano *et al*., 2000), suggesting that mitotic MEK1 signaling causes unlinking of Golgi cisternae. Recently, we found that linking of Golgi membranes into a ribbon structure depends on GM130/GRASP65 complexes (Puthenveedu *et al*., 2006). Therefore, we tested whether unlinking of the Golgi by GRASP65 knockdown rescues the M-phase delay conferred by MEK1 inhibition. GRASP65 knockdown was carried out as described previously (Puthenveedu *et al*., 2006) and led to an ~70% reduction in protein levels (Figure 3A) as well as unlinking of the Golgi ribbon (our unpublished data). In agreement with the delay observed above, U0126 treatment also caused a significant delay in cells treated with control siRNA. These cells progressed through mitosis in a cohort that peaked at 10 h after S-phase release (Figure 3B, squares). In contrast, cells treated with GRASP65 siRNA were unaffected by MEK inhibition. That is, despite the presence of U0126 the mitotic index peak for cells lacking GRASP65 (Figure 3B, triangles) was identical to

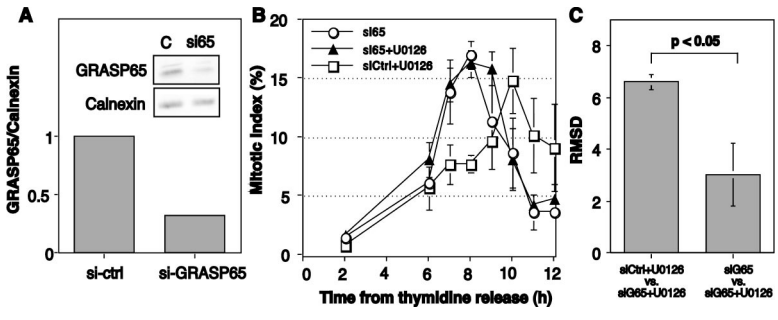

Figure 3. GRASP65 depletion suppresses the MEK1 G2/M requirement. (A) Cell extracts (40 μg/lane) prepared 72 h after transfection with GRASP65 siRNA were analyzed by immunoblotting by using anti-GRASP65 (top) and anti-calnexin (bottom) antibodies. (B) The mitotic index of control and GRASP65 siRNA-transfected cells was determined at time points after release in the presence of U0126 or 0.1% DMSO carrier added at the 2-h time point (arrow). Values shown are averages ± SEM (n = 3). Note that the delay caused by MEK inhibition was absent in cells depleted of GRASP65. (C) Also shown is the RMSD comparison of the deviation between mitotic progression curves as indicated.

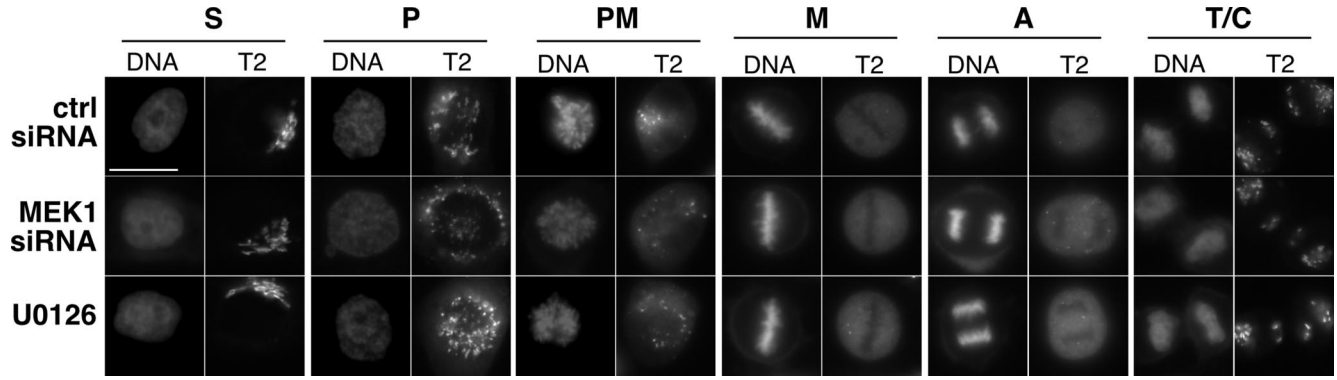

Figure 4. Mitotic Golgi disassembly does not require MEK. The Golgi and DNA patterns are shown in representative images of synchronized cells treated with control siRNA (top row), MEK1 siRNA (middle row), or 10 μM U0126 (bottom row) at the following cell cycle stages: S phase (S), prophase (P), prometaphase (PM), metaphase (M), anaphase (A), and telophase/cytokinesis (T/C).

GRASP65 knockdown cells in the absence of U0126 (Figure 3B, circles). These effects were also confirmed by RMSD analysis (Figure 3C). Our analysis did not explicitly analyze spindle morphology; therefore, we cannot rule out the possibility that spindle defects were present after GRASP65 knockdown (Sutterlin *et al*., 2005). However, the replicated experiments showed normal M-phase entry and exit without evidence of apoptosis. Possibly the S-phase arrest protected the cells from the accumulation of defects that may occur as a consequence of repeated division in the absence of GRASP65. Toward an independent confirmation of these results, we also analyzed cells after GM130 knockdown. The knockdown was carried out under conditions identical to our previous work (Puthenveedu *et al*., 2006) and yielded the expected unlinking of the Golgi ribbon. Similar to the results for GRASP65 knockdown, these cells exhibited essentially identical M-phase entry kinetics in the absence or presence of U0126 (Supplemental Figure S1). Thus, the mitotic delay caused by MEK1 inhibition seems to act through a sustained Golgi ribbon whose unlinking is necessary for normal G_2/M kinetics.

MEK Promotes Golgi Unlinking before Prophase

As described above, MEK1 mediates mitotic Golgi disassembly in permeabilized cells (Acharya *et al*., 1998), but in intact cells it may not be required (Draviam *et al*., 2001). Alternatively, its role in vivo in Golgi disassembly may not have been adequately tested due to ERK-independent activities (Colanzi *et al*., 2000) or its upstream role in cell cycle progression (Roovers and Assoian, 2000). Therefore, it was important to assay mitotic Golgi disassembly after MEK1 knockdown. Because absence of MEK1 protein or activity delayed rather than blocked mitotic progression, cells were readily identified at each M-phase stage. Significantly, compared with corresponding prophase, prometaphase, metaphase, anaphase, and telophase control cells (Figure 4, top row), Golgi organization was essentially identical in cells after either MEK1 knockdown (Figure 4, middle row) or MEK inhibition by U0126 (Figure 4, bottom row). This result indicates that although it may play a facilitating role, MEK1 is not required for mitotic Golgi disassembly.

Next, we considered the possibility that MEK1 controls G_2/M by exerting its effect on the Golgi in late G_2 phase rather than at M phase and that once M phase is reached a parallel or redundant pathway, possibly CDK-mediated Golgi vesiculation, takes over. As an initial test, we carried out live imaging of the Golgi apparatus in synchronized cells as they progressed into M phase. Consistent with previous work, characteristic features emerged from the generated movies (see Supplemental Figure S2 movie for an example). At ~7 h after release, the Golgi persisted for some time as an essentially intact ribbon (Figure 5A). Then, over a

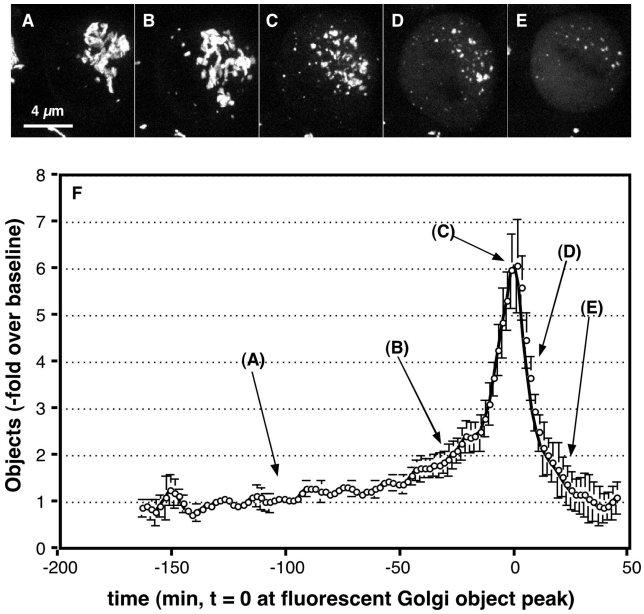

Figure 5. Live imaging analysis of mitotic Golgi disassembly. (A–E) Synchronized HeLa cells stably expressing GalNAcT2-GFP were imaged by confocal microscopy at 37°C every 2 min (10 Z-axis slices per frame). Single frames from a movie are shown representing the starting Golgi ribbon (A), initial unlinking of the ribbon (B), final unlinking yielding the peak in fluorescent objects (C), initial conversion of fragments into vesicular haze (D), and end point of disassembly with metaphase plate outlined by vesicular haze (E). (F) Frame by frame analysis of multiple movies was carried out to determine the number fluorescent Golgi objects per cell. Values are normalized by plotting the fold increase over the baseline determined for each movie (average value of first 10 frames), and the plots are aligned in time by setting t = 0 at the fluorescent Golgi object peak. Values shown are averages ± SEM (n = 10), and the approximate position of the representative stages in breakdown is indicated. Note that initial Golgi unlinking marked by the shoulder preceding the disassembly peak (B) begins greater than 60 min before metaphase (E), placing this event in late G_2 phase.

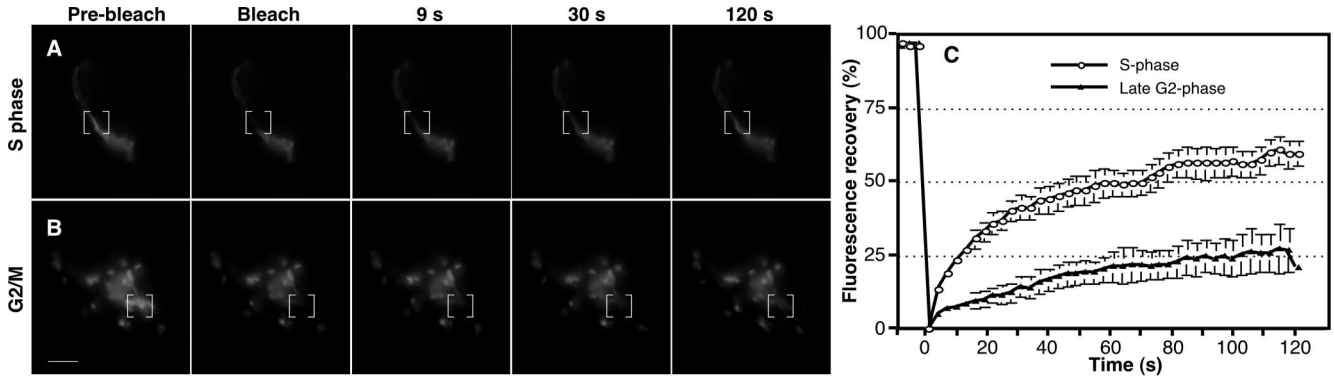

Figure 6. Decreased lateral mobility of GalNAcT2-GFP in late G_2 cells. (A and B) Synchronized HeLa cells stably expressing GalNAcT2-GFP were arrested at S phase (A) by using thymidine or arrested in late G_2 (B) by using olomoucine II treatment during the final 6 h of an 11-h thymidine washout incubation. The area of the Golgi indicated by the brackets was bleached by using a single laser pulse. Recovery of fluorescence was observed by live epifluorescence imaging (movies in Supplemental Figures S3 and S4). Representative images of the indicated time points are shown. Bar, 5 μm. (C) The ratio of fluorescence of the bleached area to an adjacent unbleached area was measured for each time point, normalized to the initial values, and plotted. Values shown are averages ± SEM (n = 3, ≥6 cells per treatment per experiment).

period of at least 30 min, the ribbon became progressively more fragmented (Figure 5B). This was followed by an abrupt period lasting ~15 min in which many small fragments were generated (Figure 5C). Over the next 10 min, these fragments underwent further breakdown becoming fluorescent haze (Figure 5D). Coincident with the rise in fluorescent haze, the outline of the metaphase plate could be seen (Figure 5E). Finally, anaphase occurred followed by reappearance of Golgi fragments and reassembly of the Golgi ribbon in the daughter cells. Individual frames from multiple movies were analyzed to determine the number of above-threshold fluorescent Golgi elements per cell, and the results are presented (Figure 5F). Importantly, the presence of a fairly prolonged stage in which Golgi elements seem to unlink from one another is a significant feature in the graph (5B). Furthermore, given that the entire prophase-to-metaphase portion of M phase usually occurs in <30 min it follows that the unlinking stage is initiated before prophase.

Golgi unlinking just before prophase was also indicated by fluorescence recovery after photobleaching (FRAP) carried out on the Golgi apparatus of S-phase and late G_2-phase cells. When a specific Golgi region is photobleached, an intact Golgi ribbon yields rapid recovery, whereas an unlinked ribbon does not (Puthenveedu *et al*., 2006). Thymidine treatment was used to accumulate S-phase cells. As expected, the Golgi ribbon was intact in S-phase cells, and green fluorescent protein (GFP)-labeled GalNacT2 rapidly recovered after photobleaching (Figure 6, A, C, and Supplemental Figure S3 movie). To accumulate late G_2 cells, thymidine washout was carried out in the presence of the CDK1 inhibitor olomoucine II (Krystof *et al*., 2005), which induced the expected arrest just before M phase (Keryer *et al*., 1998). Importantly, in late G_2 cells the ribbon was significantly fragmented (quantified below), and there was impaired fluorescence recovery even when the photobleaching was carried out on a region in proximity to other Golgi structures (Figure 6, B and C, and Supplemental Figure S4 movie). Thus, both live imaging of the Golgi in dividing cells and FRAP analysis of late G_2-arrested cells provided evidence that Golgi unlinking is taking place just before prophase.

To confirm this, we needed a way to identify the beginning of prophase; thus, we turned to analysis of Golgi linking in synchronized cells after fixation. Cells were fixed at a time point corresponding to mitotic entry for the bulk population (8–9 h postthymidine release) and stained using the Hoechst DNA stain and an anti-phospho-histone H3 antibody. Based on the time of fixation, the nonmitotic cells in the population were considered late G_2 phase cells. Importantly, the phosphorylated histone staining yielded weak but specific punctate staining in early prophase cells, providing a sensitive measure to identify and exclude these cells. To assess Golgi linking we used an objective determination of discrete Golgi elements as marked by stably expressed GFP-labeled GalNacT2 (Puthenveedu *et al*., 2006). Cells were selected solely on the basis of DNA staining, image capture and analysis used identical parameters, and final reported values are averages of independent experiments. Because Golgi ribbon formation in HeLa cells links most adjacent ministacks, there are only approximately three to four such discrete elements, on average, in control cells (Puthenveedu *et al*., 2006). Indeed, the characteristic Golgi ribbon was evident in S-phase cells (3 h postthymidine release), and quantification yielded an average of four objects per cell (Figure 7, A and B, S phase). In contrast, many late G_2 cells exhibited an unlinked appearance, and there was a significant increase in discrete Golgi elements (Figure 7, A and B, late G_2). Furthermore, the average value likely underestimates the extent of Golgi unlinking in late G_2 cells. A fraction of the cells exhibited normal ribbons. Due to incomplete synchrony in cell cycle progression, these cells may be in mid- rather than late G_2 (Figure 7C, ≤4 fragments/cell). Thus, measurable Golgi unlinking takes place before the earliest indication of CDK1 activation.

To test the role of MEK1 and CDK1 in late G_2 Golgi unlinking, we inhibited these kinases with U0126 and olomoucine II, respectively. Strikingly, in the presence of U0126, late G_2 cells exhibited linked rather than unlinked Golgi elements, and the number of discrete elements matched control values (Figure 7, A–C, late G_2 + U0126), indicating that MEK1 activity is required for Golgi unlinking in late G_2. Furthermore, olomoucine II treatment, which induced the expected arrest in late G_2 (Keryer *et al*., 1998), left the Golgi unlinked (Figure 7, A and B, Olo arrest). But if the olomoucine II arrest was carried out on cells pretreated with U0126, the Golgi remained linked (Figure 7, A and B, Olo arrest + U0126). MEK-dependent, G_2 Golgi unlinking

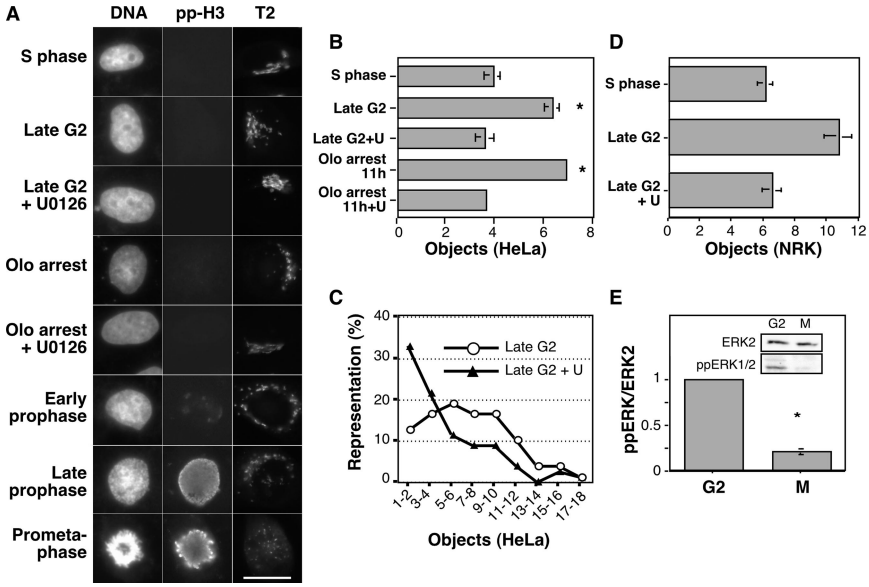

Figure 7. MEK-dependent Golgi unlinking before prophase. (A) Representative images show Hoechst-labeled DNA (left column), phosphohistone H3 immunofluorescence (center column) and the Golgi apparatus labeled by GalNAcT2-GFP (T2, right column) after fixation at the designated cell cycle stages, as determined by time from cell cycle release, DNA condensation status and the presence or absence of pp-H3 staining. Where indicated U0126 was added 5 h after thymidine release, and/or 10 μM olomocine II was added 7.5 h after release, and cells were maintained in olomoucine G_2/M arrest for three more hours before fixation. (B) For quantitative analysis of Golgi linking in the populations shown in A, the NIH Image software package was used to automatically apply a threshold and count above-threshold fluorescent objects. Note that the analyzed cells were chosen on the basis of interphase DNA staining and not Golgi pattern. Average values ± SEM are shown (n = 3). (C) Histogram analysis showing the percentage of cells exhibiting the indicated number of Golgi fragments for control and U0126-treated late G_2 cells. (D) Analysis of Golgi linking was carried out on synchronized NRK cells exactly as described for HeLa cells except that giantin immunofluorescence was used to visualize the Golgi apparatus. (E) Synchronized HeLa cells were subjected to shake off at a time corresponding to mitotic entry (8–9 h). Extracts (50 μg/lane) of the adherent (G_2-phase) and released (M-phase) cells were analyzed for doubly phosphorylated ERK1/2 by immunoblotting. After stripping, the blot was reprobed to detect ERK2 as a loading control. Quantified values normalized by the ERK2 loading control are averages ± SEM (n = 3).

was also observed in a distinct cell type. Synchronized normal rat kidney (NRK) cells were analyzed using anti-giantin immunostaining, and the G_2 population of cells exhibited a significant increase in unlinked Golgi elements compared with the S-phase population, but this increase was absent if U0126 was added to inhibit MEK activity (Figure 7D). We also confirmed that MEK is actually active in late G_2 phase by determination of cellular levels of doubly phosphorylated ERK1/2. Synchronized cells beginning to enter M phase (8–9 h postthymidine release) were subjected to shake-off followed by immunoassay of the remaining adherent cells, which were nonmitotic and, based on the time point, assumed to be in late G_2 phase. For comparison, the released mitotic cells were collected and also assayed. Doubly phosphorylated ERK1/2 was clearly evident in the G_2 population, and the level was significantly higher than in the mitotic population (Figure 7E). Thus, consistent with a previous analysis (Roberts *et al*., 2002), MEK is active in G_2 phase. Altogether these findings indicate that MEK1, but not CDK1, is required for Golgi unlinking and that unlinking takes place in late G_2 before CDK1 activation.

If Golgi linking status in late G_2 influences CDK1 activation, then cells with a linked Golgi might show a delay in CDK1 activation upon release from the G_2/M arrest imposed by olomoucine treatment. Indeed, a direct comparison showed that, upon olomoucine washout, cells pretreated with U0126 to prevent Golgi unlinking persisted in early prophase significantly longer than control cells with an unlinked Golgi (Figure 8A). Evidence that this effect related to Golgi structure rather than a Golgi independent MEK1 pathway was provided by BFA-mediated Golgi disassembly. That is, treatment of cells with BFA rescued the delay, allowing normal progression into later M-phase stages (Figure 8B). Together, these results demonstrate that the onset of mitosis driven by full activation of CDK1 involves unlinking of the Golgi apparatus in late G_2 by MEK signaling.

Evidence That GRASP55 Phosphorylation Plays a Role in Normal Mitotic Progression

To test whether the Golgi-localized MEK pathway target GRASP55 might be involved, we expressed myc-tagged GRASP55-T222,225A, a version that we previously showed fails to undergo MEK-dependent phosphorylation by ERK (Jesch *et al*., 2001a), and we assayed Golgi linking and progression into M phase. As a control, the corresponding myc-tagged wild-type GRASP55 was also expressed. Both constructs exhibited similar transfection frequencies and were

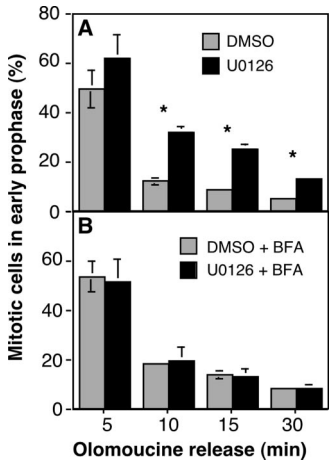

Figure 8. MEK inhibition prolongs mitotic entry. (A) HeLa cells were released from an arrest with 10 μM olomoucine II carried out in the presence of either U0126 or DMSO carrier. At time points after release, in the continued presence of U0126 or DMSO, the percentage of ppH3-positive cells in early prophase (weak punctate staining) was determined. (B) The experiment was performed identically except that 2 μM BFA was added 30 min before olomoucine release. Average values ± SEM are shown (n = 3).

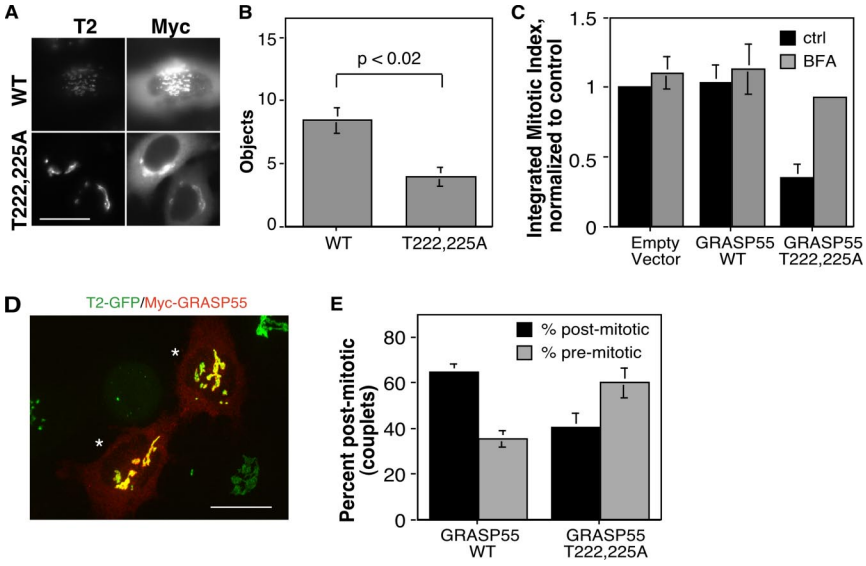

Figure 9. Evidence that GRASP55 phosphorylation is required for timely G_2/M. (A) Myc-GRASP55 (WT) and the myc-GRASP55$_{T222,225A}$ phosphorylation mutant (T222,225A) were transiently expressed, and the cells were synchronized in late G_2 phase by using a 11-h thymidine release incubation in the presence of olomoucine II starting at 6 h. Expressing cells were identified by myc staining (Myc), and the Golgi was analyzed based on GalNAcT2-GFP (T2). (B) Golgi linking in the olomoucine-arrested cells expressing myc-GRASP55 or myc-GRASP55$_{T222,225A}$, was then quantified by determining the number of fluorescent Golgi objects per cell (n = 3, ≥25 cells per treatment per experiment). (C) The integrated total percentage of visibly mitotic cells after S-phase release was determined for cells transfected with empty vector, or vectors encoding GRASP55 and GRASP55$_{T222,225A}$. Also shown are the results obtained when BFA was added at 5 h after S-phase release to cause Golgi disassembly. All values are normalized to the empty vector control. Expression of GRASP55$_{T222,225A}$ decreased mitotic entry and this was suppressed by BFA addition. (D) Representative post mitotic couplet expressing myc-GRASP55 is shown (asterisks) after staining with anti-myc (red) and visualizing GalNAcT2-GFP (green). Bar, 4 μm. (E) Percentage of premitotic (singlets) and postmitotic (couplets) cells was determined 2 h after mitotic entry for cells expressing GRASP55 or GRASP55$_{T222,225A}$. Expression-positive mitotic cells were included in the postmitotic count but were rarely observed due to diminished staining upon Golgi dispersal. Average values ± SEM are shown (n = 3). In comparison with GRASP55, recovery of postmitotic cells was dramatically reduced by GRASP55$_{T222,225A}$ expression ($p < 0.05$).

Golgi localized as indicated by colocalization with the Golgi marker GPP130 (our unpublished observations). If GRASP55 phosphorylation is required for late G_2 Golgi unlinking, then the Golgi may fail to unlink in cells expressing GRASP55-T222,225A. As a test we assayed Golgi linking in olomoucine II arrested late G_2 cells. As shown above (Figure 7), control cells exhibited significant unlinking of the Golgi ribbon in late G_2 phase, and this was also the case for cells expressing wild-type GRASP55 (Figure 9A, WT). In contrast, cells expressing GRASP55-T222,225A had intact Golgi ribbons (Figure 9A, T222,225A). This was supported by quantification of fluorescent Golgi objects in numerous wild-type– and GRASP55-T222,225A–expressing cells over several experiments (Figure 9B). GRASP55-T222,225A expression suppressed late G_2 Golgi unlinking to levels equaling that present in S-phase control cells, suggesting that GRASP55 phosphorylation is required for Golgi unlinking.

Furthermore, whereas expression of wild-type GRASP55 had no effect on progression into M phase, as indicated by comparison with cells transfected with empty vector, cells expressing GRASP55-T222,225A showed a profound inhibition in mitotic entry (Figure 9C). Inhibition of G_2/M corresponded to the transfection frequency and was uniform across multiple experiments ($p < 0.05$, n = 3). As a further control for this experiment, we attempted to rescue the inhibition imposed by GRASP55-T222,225A expression using forced Golgi dispersal by BFA. BFA addition had no significant effect on either the empty vector or the wild-type–transfected controls; however, it almost completely restored normal mitotic progression to GRASP55-T222,225A–transfected cells (Figure 9C). Thus, the requirement for GRASP55 phosphorylation can be bypassed by dispersing the Golgi by other means. As an additional test, we allowed synchronized cells to pass through mitosis, and then ~2 h postmitotic entry, a time more than sufficient to move through cytokinesis, we determined the percentage of GRASP55-expressing cells that had completed mitosis. These daughter cells, which were counted as single couplets, were identified on the basis of their contact, size, and expression level (Figure 9D). Consistent with a delay caused by preventing GRASP55 phosphorylation, there was a dramatic reduction in recovery of couplets expressing GRASP55 T222,225A compared with wild-type (Figure 9E). In sum, the results indicate that MEK signaling promotes G_2/M by unlinking the Golgi and that this involves, at least in part, phosphorylation of GRASP55.

DISCUSSION

The role of MEK1 at the G_2/M transition of the cell cycle has remained unclear, particularly in light of conflicting reports concerning MEK1 and mitotic Golgi disassembly (Acharya *et al*., 1998; Lowe *et al*., 1998; Draviam *et al*., 2001; Colanzi *et al*., 2003b). Consistent with recent work (Wright *et al*., 1999; Roberts *et al*., 2002), we found that MEK1 inhibition delayed progression into M phase, indicating that MEK signaling, although not absolutely necessary, is required for timely G_2/M. Significantly, this requirement is shown here for the first time to be bypassed by prior disassembly or unlinking of the Golgi apparatus, suggesting that MEK acts to unlink the Golgi and that the previously described Golgi checkpoint (Sutterlin *et al*., 2002) is, in fact, controlled by MEK signaling. Furthermore, MEK-dependent unlinking of the Golgi apparatus occurred before prophase in late G_2 and phosphorylation of the MEK1 Golgi target GRASP55 seemed to be important for both Golgi unlinking and mitotic entry. These results establish a cell cycle role for MEK signaling in late G_2 and suggest that MEK, by activating ERK, induces phosphorylation of GRASP55, thereby unlinking the Golgi apparatus. The unlinked Golgi apparatus then facilitates progression into M phase, perhaps via release and/or dispersal of CDK1 activators.

The finding that MEK1-mediated Golgi rearrangement facilitates G_2/M uncovers a previously unestablished link between work on connections between the Golgi apparatus and G_2/M on one hand and work on MEK1 and the Golgi apparatus on the other hand. The presence of a G_2/M checkpoint sensitive to Golgi structure was suggested by the

ability of dominant-negative or antibody inhibitors against GRASP65 to arrest or delay the G_2/M transition (Sutterlin *et al*., 2002). Importantly, this effect is nullified in cells with a disassembled Golgi apparatus. Although GRASP65 itself is not required in vivo for either mitotic entry or mitotic Golgi disassembly (Figure 3; Sutterlin *et al*., 2005), it is required to link the Golgi apparatus into a ribbon (Puthenveedu *et al*., 2006), suggesting that it is the persistence of a linked Golgi apparatus that delays mitotic entry. These observations concerning GRASP65 suggested a connection to MEK1 activity at G_2/M because MEK1-activated ERK2 mitotically phosphorylates the closely related GRASP55 (Jesch *et al*., 2001a). Furthermore, MEK1 mediates in vitro mitotic Golgi fragmentation (Acharya *et al*., 1998), and MEK1 has been implicated in G_2/M (Wright *et al*., 1999; Roberts *et al*., 2002). Also, it was recently found that ERK1c knockdown delays mitotic progression and Golgi breakdown, but a causal link between these effects was not tested (Shaul and Seger, 2006). This connection is now strengthened by our demonstration that MEK signaling controls Golgi structure in vivo and that Golgi unlinking bypasses MEK1 control of G_2/M.

A puzzling implication of the Golgi checkpoint, as defined previously, is that it requires Golgi disassembly to be both a cause and a consequence of the G_2/M transition. Our finding that the Golgi undergoes MEK-dependent rearrangement before prophase resolves this apparent paradox. That is, MEK1 unlinks the Golgi in preparation for G_2/M and this unlinking may facilitate CDK1 activation. Active CDK1 is then presumably sufficient to promote full mitotic vesiculation of the Golgi. This scenario fits well with previous work. MEK1/ERKs are active in late G_2 and M phase (Shapiro *et al*., 1998; Colanzi *et al*., 2000; Hayne *et al*., 2000; Roberts *et al*., 2002; Shaul and Seger, 2006), and in a permeabilized cell assay, both MEK1 and CDK1 can induce Golgi reorganization, but MEK1 acts upstream of CDK1 (Kano *et al*., 2000). Moreover, in this assay MEK1 fragments the Golgi apparatus, whereas CDK1, perhaps acting directly on vesicle trafficking targets, induces Golgi vesiculation. The initiation of MEK1-dependent Golgi unlinking before prophase clarifies why it might be considered a cause of G_2/M in that it facilitates the transition, whereas CDK1-dependent Golgi vesiculation is a consequence of G_2/M. That MEK1 acts in late G_2 to regulate Golgi organization and to exert control over G_2/M strongly suggests that MEK1 is, indeed, playing a role in G_2/M control.

What is the function of the putative MEK1/Golgi checkpoint? That is, what triggers MEK1 signaling in late G_2 and why? Immediately upstream of MEK1 is likely Raf1 (Colanzi *et al*., 2003b), but the key question is the ultimate origin of the signal. Growth factor-induced signaling seems unlikely. After commitment to S phase, the cell cycle is independent of growth factors, and, at least in M phase, MEK1/2 is uncoupled from growth factor receptors (Dangi and Shapiro, 2005). Furthermore, there is no evidence that Golgi structure, the identified target of late G_2 MEK signaling, is controlled by growth factor/MAP kinase signaling at other cell cycle stages. Perhaps the purpose of late G_2 Golgi unlinking is to ensure accurate Golgi inheritance (Acharya *et al*., 1998; Colanzi *et al*., 2003a). A linked Golgi opposes the Golgi membrane partitioning mechanism, which seems to involve membrane dispersal (Lucocq *et al*., 1987; Jesch *et al*., 2001b). Although the subsequent mitotic Golgi breakdown would seem sufficient for accurate partitioning, the late G_2 Golgi unlinking reaction may have evolved because it uniquely allows a premitosis check on the status of Golgi dispersal. Another possibility is that the pathway is connected to centrosome duplication and activation. During interphase, Golgi ribbons are positioned adjacent to, and may be physically linked to, centrosomes actively involved in nucleating microtubule assembly (for reviews, see Rios and Bornens, 2003; Linstedt, 2004). In preparation for mitosis, centrosome duplication and separation are required steps before CDK1 activation (Lindqvist *et al*., 2005). A linked Golgi apparatus may impede centrosome separation, and this, in turn, might cause a delay in G_2/M. Thus, under normal conditions, centrosome duplication might generate a signal activating MEK1, which, via Golgi unlinking, promotes centrosome separation. Another possibility is that MEK1 is involved in size control. In yeast, G_2/M progression depends on a cell size checkpoint. Although direct coupling of cell size and cell cycle progression is uncertain in mammals (Tapon *et al*., 2001), the idea is intriguing given that the Golgi apparatus influences cell size via its contribution of membrane to the cell surface. The Golgi itself must double each cell cycle in preparation for cell division. Perhaps MEK1 signaling assembled on the Golgi apparatus by the Sef1 scaffold (Torii *et al*., 2004a) is sensitive to size or growth rate and this impinges on Golgi substrates, such as GRASP55, to unlink the Golgi ribbon for the purpose of centrosome separation and/or the release promitotic factors.

In addition to lateral cross-bridging of Golgi ministacks, GM130/GRASP65 complexes, and possibly golgin45/GRASP55 complexes, also associate with numerous factors on the cytoplasmic face of the Golgi apparatus, including the protein kinases Ysk1, Mst4, and PLK1 (Preisinger *et al*., 2004; Preisinger *et al*., 2005). Regulation of these associated factors, rather than Golgi unlinking per se, may be the mechanism facilitating G_2/M. For example, phosphorylation of GRASP proteins may release and activate components that impinge on cdc25 activation of CDK1. Alternatively, Golgi signaling factors may remain membrane associated, and it may be the location of the membranes that is regulated. Dispersed Golgi ministacks is actually the normal state in most nonmammalian cell types, and these may function as distributive signaling centers for G_2/M progression. By this reasoning, the Golgi ribbon would be unlinked in mammalian cells in late G_2 to recapitulate this distributive signaling.

In sum, MEK1 signaling is active before prophase to unlink the Golgi apparatus and promote the G_2/M transition. Further work may reveal that MEK-dependent phosphorylation of GRASP55 regulates Golgi inheritance, centrosome separation, or possibly a cell size checkpoint. These findings begin to elucidate key mechanistic aspects of the control by a secretory organelle over a fundamentally important cell cycle transition.

ACKNOWLEDGMENTS

We thank Dr. Manojkumar Puthenveedu for critical suggestions, Dr. Fred Lanni for generous contribution of resources for the photobleaching experiments, and members of the Linstedt laboratory and the anonymous reviewers for suggesting improvements to the study. Funding was provided by grants RSG-03-148-01-CSM and GM-56779 (to A.D.L.).

REFERENCES

Abrieu, A., Fisher, D., Simon, M. N., Doree, M., and Picard, A. (1997). MAPK inactivation is required for the G2 to M-phase transition of the first mitotic cell cycle. EMBO J. *16*, 6407–6413.

Acharya, U., Mallabiabarrena, A., Acharya, J. K., and Malhotra, V. (1998). Signaling via mitogen-activated protein kinase kinase (MEK1) is required for Golgi fragmentation during mitosis. Cell *92*, 183–192.

Bachert, C., Lee, T. H., and Linstedt, A. D. (2001). Lumenal endosomal and Golgi-retrieval determinants involved in pH-sensitive targeting of an early Golgi protein. Mol. Biol. Cell *12*, 3152–3160.

Besson, A., Davy, A., Robbins, S. M., and Yong, V. W. (2001). Differential activation of ERKs to focal adhesions by PKC epsilon is required for PMA-induced adhesion and migration of human glioma cells. Oncogene *20*, 7398–7407.

Bitangcol, J. C., Chau, A. S., Stadnick, E., Lohka, M. J., Dicken, B., and Shibuya, E. K. (1998). Activation of the p42 mitogen-activated protein kinase pathway inhibits Cdc2 activation and entry into M-phase in cycling *Xenopus* egg extracts. Mol. Biol. Cell *9*, 451–467.

Chung, E., and Chen, R. H. (2003). Phosphorylation of Cdc20 is required for its inhibition by the spindle checkpoint. Nat. Cell Biol. *5*, 748–753.

Colanzi, A., Deerinck, T. J., Ellisman, M. H., and Malhotra, V. (2000). A specific activation of the mitogen-activated protein kinase kinase 1 (MEK1) is required for Golgi fragmentation during mitosis. J. Cell Biol. *149*, 331–339.

Colanzi, A., Suetterlin, C., and Malhotra, V. (2003a). Cell-cycle-specific Golgi fragmentation: how and why? Curr. Opin. Cell Biol. *15*, 462–467.

Colanzi, A., Sutterlin, C., and Malhotra, V. (2003b). RAF1-activated MEK1 is found on the Golgi apparatus in late prophase and is required for Golgi complex fragmentation in mitosis. J. Cell Biol. *161*, 27–32.

Dangi, S., and Shapiro, P. (2005). Cdc2-mediated inhibition of epidermal growth factor activation of the extracellular signal-regulated kinase pathway during mitosis. J. Biol. Chem. *280*, 24524–24531.

Draviam, V. M., Orrechia, S., Lowe, M., Pardi, R., and Pines, J. (2001). The localization of human cyclins B1 and B2 determines CDK1 substrate specificity and neither enzyme requires MEK to disassemble the Golgi apparatus. J. Cell Biol. *152*, 945–958.

Harding, A., Giles, N., Burgess, A., Hancock, J. F., and Gabrielli, B. G. (2003). Mechanism of mitosis-specific activation of MEK1. J. Biol. Chem. *278*, 16747–16754.

Hayne, C., Tzivion, G., and Luo, Z. (2000). Raf-1/MEK/MAPK pathway is necessary for the G2/M transition induced by nocodazole. J. Biol. Chem. *275*, 31876–1882.

Hayne, C., Xiang, X., and Luo, Z. (2004). MEK inhibition and phosphorylation of serine 4 on B23 are two coincident events in mitosis. Biochem. Biophys. Res. Commun. *321*, 675–680.

Hidalgo Carcedo, C., Bonazzi, M., Spano, S., Turacchio, G., Colanzi, A., Luini, A., and Corda, D. (2004). Mitotic Golgi partitioning is driven by the membrane-fissioning protein CtBP3/BARS. Science *305*, 93–96.

Horne, M. M., and Guadagno, T. M. (2003). A requirement for MAP kinase in the assembly and maintenance of the mitotic spindle. J. Cell Biol. *161*, 1021–1028.

Itoh, T., Yamauchi, A., Miyai, A., Yokoyama, K., Kamada, T., Ueda, N., and Fujiwara, Y. (1994). Mitogen-activated protein kinase and its activator are regulated by hypertonic stress in Madin-Darby canine kidney cells. J. Clin. Invest *93*, 2387–2392.

Jesch, S. A., Lewis, T. S., Ahn, N. G., and Linstedt, A. D. (2001a). Mitotic phosphorylation of Golgi reassembly stacking protein 55 by mitogen-activated protein kinase ERK2. Mol. Biol. Cell *12*, 1811–1817.

Jesch, S. A., and Linstedt, A. D. (1998). The Golgi and endoplasmic reticulum remain independent during mitosis in HeLa cells. Mol. Biol. Cell *9*, 623–635.

Jesch, S. A., Mehta, A. J., Velliste, M., Murphy, R. F., and Linstedt, A. D. (2001b). Mitotic Golgi is in a dynamic equilibrium between clustered and free vesicles independent of the ER. Traffic *2*, 873–884.

Kano, F., Takenaka, K., Yamamoto, A., Nagayama, K., Nishida, E., and Murata, M. (2000). MEK and Cdc2 kinase are sequentially required for Golgi disassembly in MDCK cells by the mitotic *Xenopus* extracts. J. Cell Biol. *149*, 357–368.

Keryer, G., Yassenko, M., Labbe, J. C., Castro, A., Lohmann, S. M., Evain-Brion, D., and Tasken, K. (1998). Mitosis-specific phosphorylation and subcellular redistribution of the RIIalpha regulatory subunit of cAMP-dependent protein kinase. J. Biol. Chem. *273*, 34594–34602.

Krystof, V., McNae, I. W., Walkinshaw, M. D., Fischer, P. M., Muller, P., Vojtesek, B., Orsag, M., Havlicek, L., and Strnad, M. (2005). Antiproliferative activity of olomoucine II, a novel 2,6,9-trisubstituted purine cyclin-dependent kinase inhibitor. Cell Mol. Life Sci. *62*, 1763–1771.

Lindqvist, A., Kallstrom, H., Lundgren, A., Barsoum, E., and Rosenthal, C. K. (2005). Cdc25B cooperates with Cdc25A to induce mitosis but has a unique role in activating cyclin B1-Cdk1 at the centrosome. J. Cell Biol. *171*, 35–45.

Linstedt, A. D. (2004). Positioning the Golgi apparatus. Cell *118*, 271–272.

Linstedt, A. D., and Hauri, H. P. (1993). Giantin, a novel conserved Golgi membrane protein containing a cytoplasmic domain of at least 350 kDa. Mol. Biol. Cell *4*, 679–693.

Linstedt, A. D., Mehta, A., Suhan, J., Reggio, H., and Hauri, H. P. (1997). Sequence and overexpression of GPP130/GIMPc: evidence for saturable pH-sensitive targeting of a type II early Golgi membrane protein. Mol. Biol. Cell *8*, 1073–1087.

Lippincott-Schwartz, J., Yuan, L. C., Bonifacino, J. S., and Klausner, R. D. (1989). Rapid redistribution of Golgi proteins into the ER in cells treated with brefeldin A: evidence for membrane cycling from Golgi to ER. Cell *56*, 801–813.

Liu, X., Yan, S., Zhou, T., Terada, Y., and Erikson, R. L. (2004). The MAP kinase pathway is required for entry into mitosis and cell survival. Oncogene *23*, 763–776.

Lou, Y., Xie, W., Zhang, D. F., Yao, J. H., Luo, Z. F., Wang, Y. Z., Shi, Y. Y., and Yao, X. B. (2004). Nek2A specifies the centrosomal localization of Erk2. Biochem. Biophys. Res. Commun. *321*, 495–501.

Lowe, M., Rabouille, C., Nakamura, N., Watson, R., Jackman, M., Jamsa, E., Rahman, D., Pappin, D. J., and Warren, G. (1998). Cdc2 kinase directly phosphorylates the cis-Golgi matrix protein GM130 and is required for Golgi fragmentation in mitosis. Cell *94*, 783–793.

Lucocq, J. M., Pryde, J. G., Berger, E. G., and Warren, G. (1987). A mitotic form of the Golgi apparatus in HeLa cells. J. Cell Biol. *104*, 865–874.

Mansour, S. J., Matten, W. T., Hermann, A. S., Candia, J. M., Rong, S., Fukasawa, K., Vande Woude, G. F., and Ahn, N. G. (1994). Transformation of mammalian cells by constitutively active MAP kinase kinase. Science *265*, 966–970.

Minshull, J., Sun, H., Tonks, N. K., and Murray, A. W. (1994). A MAP kinase-dependent spindle assembly checkpoint in *Xenopus* egg extracts. Cell *79*, 475–486.

Misteli, T., and Warren, G. (1995). Mitotic disassembly of the Golgi apparatus in vivo. J. Cell Sci. *108*, 2715–2727.

Murakami, M. S., and Vande Woude, G. F. (1998). Analysis of the early embryonic cell cycles of *Xenopus*; regulation of cell cycle length by Xe-wee1 and Mos. Development *125*, 237–248.

Peyroche, A., Antonny, B., Robineau, S., Acker, J., Cherfils, J., and Jackson, C. L. (1999). Brefeldin A acts to stabilize an abortive ARF-GDP-Sec7 domain protein complex: involvement of specific residues of the Sec7 domain. Mol. Cell *3*, 275–285.

Preisinger, C., Korner, R., Wind, M., Lehmann, W. D., Kopajtich, R., and Barr, F. A. (2005). Plk1 docking to GRASP65 phosphorylated by Cdk1 suggests a mechanism for Golgi checkpoint signalling. EMBO J. *24*, 753–765.

Preisinger, C., Short, B., De Corte, V., Bruyneel, E., Haas, A., Kopajtich, R., Gettemans, J., and Barr, F. A. (2004). YSK1 is activated by the Golgi matrix protein GM130 and plays a role in cell migration through its substrate 14-3-3zeta. J. Cell Biol. *164*, 1009–1020.

Puthenveedu, M. A., Bachert, C., Puri, S., Lanni, F., and Linstedt, A. D. (2006). GM130 and GRASP65-dependent lateral cisternal fusion allows uniform Golgi-enzyme distribution. Nat. Cell Biol. *8*, 238–248.

Puthenveedu, M. A., and Linstedt, A. D. (2001a). Evidence that Golgi structure depends on a p115 activity that is independent of the vesicle tether components giantin and GM130. J. Cell Biol. *155*, 227–238.

Puthenveedu, M. A., and Linstedt, A. D. (2001b). In search of an essential step during mitotic Golgi disassembly and inheritance. Exp. Cell Res. *271*, 22–27.

Rios, R. M., and Bornens, M. (2003). The Golgi apparatus at the cell centre. Curr. Opin. Cell Biol. *15*, 60–66.

Roberts, E. C., Shapiro, P. S., Nahreini, T. S., Pages, G., Pouyssegur, J., and Ahn, N. G. (2002). Distinct cell cycle timing requirements for extracellular signal-regulated kinase and phosphoinositide 3-kinase signaling pathways in somatic cell mitosis. Mol. Cell. Biol. *22*, 7226–7241.

Roovers, K., and Assoian, R. K. (2000). Integrating the MAP kinase signal into the G1 phase cell cycle machinery. Bioessays *22*, 818–826.

Seemann, J., Jokitalo, E., Pypaert, M., and Warren, G. (2000). Matrix proteins can generate the higher order architecture of the Golgi apparatus. Nature *407*, 1022–1026.

Shapiro, P. S., Vaisberg, E., Hunt, A. J., Tolwinski, N. S., Whalen, A. M., McIntosh, J. R., and Ahn, N. G. (1998). Activation of the MKK/ERK pathway during somatic cell mitosis: direct interactions of active ERK with kinetochores and regulation of the mitotic 3F3/2 phosphoantigen. J. Cell Biol. *142*, 1533–1545.

Shapiro, P. S., Whalen, A. M., Tolwinski, N. S., Wilsbacher, J., Froelich-Ammon, S. J., Garcia, M., Osheroff, N., and Ahn, N. G. (1999). Extracellular signal-regulated kinase activates topoisomerase IIalpha through a mechanism independent of phosphorylation. Mol. Cell. Biol. *19*, 3551–3560.

Shaul, Y. D., and Seger, R. (2006). ERK1c regulates Golgi fragmentation during mitosis. J. Cell Biol. *172*, 885–897.

Sutterlin, C., Hsu, P., Mallabiabarrena, A., and Malhotra, V. (2002). Fragmentation and dispersal of the pericentriolar Golgi complex is required for entry into mitosis in mammalian cells. Cell *109*, 359–369.

Sutterlin, C., Polishchuk, R., Pecot, M., and Malhotra, V. (2005). The Golgi-associated protein GRASP65 regulates spindle dynamics and is essential for cell division. Mol. Biol. Cell *16*, 3211–3222.

Takenaka, K., Gotoh, Y., and Nishida, E. (1997). MAP kinase is required for the spindle assembly checkpoint but is dispensable for the normal M phase entry and exit in *Xenopus* egg cell cycle extracts. J. Cell Biol. *136*, 1091–1097.

Tapon, N., Moberg, K. H., and Hariharan, I. K. (2001). The coupling of cell growth to the cell cycle. Curr. Opin. Cell Biol. *13*, 731–737.

Torii, S., Kusakabe, M., Yamamoto, T., Maekawa, M., and Nishida, E. (2004a). Sef is a spatial regulator for Ras/MAP kinase signaling. Dev. Cell *7*, 33–44.

Torii, S., Nakayama, K., Yamamoto, T., and Nishida, E. (2004b). Regulatory mechanisms and function of ERK MAP kinases. J. Biochem. *136*, 557–561.

Ussar, S., and Voss, T. (2004). MEK1 and MEK2, different regulators of the G1/S transition. J. Biol. Chem. *279*, 43861–43869.

Walter, S. A., Guadagno, T. M., and Ferrell, J. E., Jr. (1997). Induction of a G2-phase arrest in *Xenopus* egg extracts by activation of p42 mitogen-activated protein kinase. Mol. Biol. Cell *8*, 2157–2169.

Wang, Y., Seemann, J., Pypaert, M., Shorter, J., and Warren, G. (2003). A direct role for GRASP65 as a mitotically regulated Golgi stacking factor. EMBO J. *22*, 3279–3290.

Wright, J. H., Munar, E., Jameson, D. R., Andreassen, P. R., Margolis, R. L., Seger, R., and Krebs, E. G. (1999). Mitogen-activated protein kinase kinase activity is required for the G(2)/M transition of the cell cycle in mammalian fibroblasts. Proc. Natl. Acad. Sci. USA *96*, 11335–11340.

Yoshimura, S., Yoshioka, K., Barr, F. A., Lowe, M., Nakayama, K., Ohkuma, S., and Nakamura, N. (2005). Convergence of cell cycle regulation and growth factor signals on GRASP65. J. Biol. Chem. *280*, 23048–23056.